ELSEVIER

Journal of Nuclear Materials 241–243 (1997) 1248–1252

journal of nuclear materials

Impurity generation for low energy range of ion bombardment and its transport in a plasma

M. Kojima [a,*], S. Takamura [b]

[a] *Department of Electrical Engineering, Graduate School of Engineering, Nagoya University, Nagoya 464-01, Japan*
[b] *Department of Energy Engineering and Science, Graduate School of Engineering, Nagoya University, Nagoya 464-01, Japan*

Abstract

Fundamental processes for impurity generation and its transport have been investigated by observing time-dependent spatial structures of impurity atoms and ions using an ICCD camera with high temporal resolution. In a helium plasma environment, the different energy distribution of sputtered titanium atoms is identified depending on ion bombardment energy, especially about a lack of high energy population for low incident energy range of impinging ions on the target. By comparing the experimental observations on the time evolution of ion spectral line with the spatial distribution obtained by a Monte Carlo simulation code taking account of the velocity distribution of sputtered atoms, the cross-field diffusion of impurity ions has been found to be described nearly as the classical process.

Keywords: NAGDIS-I; Divertor simulator; Monte Carlo simulation; Impurity transport; Physical erosion

1. Introduction

Linear plasma machine is useful to understand fundamental properties in plasma–surface interactions such as impurity generation, transport in a plasma, and redeposition on the surface. It has a simple magnetic structure with a well-defined plasma in steady state. Also, it is possible to obtain a low ion bombardment energy of less than 1 keV encountered in the edge plasma of fusion devices and at the same time a high ion flux $\sim 10^{20-24}$ ions m^{-2} s^{-1} compared with those in ion beam experiments. To understand the sputtering physics, several experiments have been carried out by means of a time-of-flight method [1] or laser-induced fluorescence [2,3] using an ion beam. The energy distribution of sputtered atoms derived by Thompson [4] is considered to be a good approximation for the bombarding ion energy of more than a few keV and is useful owing to its simple formula. For low ion bombardment energy (usually encountered in a divertor region), however, the energy distribution of sputtered atoms may be quite different from Thompson distribution [2].

The velocity distribution of sputtered atoms is recognized to be very important since it determines the penetration length of impurity into divertor plasma and SOL region in fusion devices. It is influenced by the mechanism of impinging ions and material atoms interactions [5]. Such impurity production processes, and subsequent transport in a plasma (cross-field diffusion, the effects of ion flow, etc.) and redeposition processes deeply affect the surface erosion of a plasma-facing material. Therefore, it is quite important to investigate individual physics in a series of impurity processes from fundamental points of view.

We have investigated impurity production and transport processes by observing the time evolution of two-dimensional profiles with a high spatial resolution. The focused points for the present study are as follows: (a) the energy distribution of sputtered atoms for different incident ion energies, particularly for low energy region, and (b) the cross-field diffusion coefficient for impurity ions. These are successfully studied with a high speed optical technique in a plasma environment using spectral line of atoms or ions induced by the plasma electron impact excitation which is impossible in ion beam experiments.

* Corresponding author. Tel.: +81-52 789 5429; fax: +81-52 789 3944; e-mail: kojima@rose.nifs.ac.jp.

PII S0022-3115(96)00708-8

2. Experimental and numerical studies

2.1. Experimental set-up on NAGDIS-I

Experiments have been carried out for a titanium target plate (9 cm^2) installed at the end of a helium plasma column in the Nagoya University Divertor Simulator (NAGDIS-I) [6] as shown in Fig. 1. Applying a pulsed negative bias to the titanium target for 10 μs, accelerated plasma ions strike the target and produce the constituent atoms by physical sputtering during that short period. The ion energy is controlled in the range from 100 eV to 600 eV. Under this situation the incidence of ions is approximately normal to the target due to the low ion temperature of a few eV and the strong sheath electric field. We can neglect any ion ejection from the target into the plasma because of the strong negative potential. The effect of self-sputtering can be considered negligible because the sputtering yield of titanium is small less than 0.05 atoms/ion during target biasing, and that the sheath potential of $\sim$ 35 eV, set before and after the biasing, is lower than the threshold energy of self-sputtering of $\sim$ 40 eV [7], so that the fraction of titanium ions in the impurity ions on the target should be quite small. Therefore, we can carry out the following fundamental experiments without any complex conditions.

Two-dimensional intensity profiles of light emission from titanium atoms (Ti I 399.9 nm) and ions (Ti II 368.5 nm) have been observed using an image intensified CCD (ICCD) camera with an interference filter. The ICCD camera has a high shuttering speed of less than 10 μs, high sensitivity and 0.7 mm/pixel as spatial resolution. The field of view is as follows: $\pm$20 mm in the vertical direction and up to 80 mm from the target surface in the horizontal direction along the magnetic field. We first make an averaged image by adding different thirty images under the same conditions, and construct a final image by subtracting the averaged image data without pulse biasing from those with biasing. A typical image of Ti I 399.9 nm, with the same time interval for the shuttering as that for the biasing pulse, is also shown in the Fig. 1.

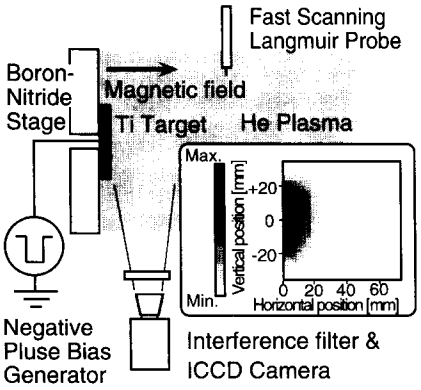

Fig. 1. Schematic diagram of experimental set up on NAGDIS-I, and a typical image taken by an ICCD camera.

2.2. Numerical model

In our numerical simulation code, test impurity atoms are traced starting from the surface of the target plate until ionized, and then newly-born impurity ions are followed by solving the equation of motion with magnetic field in a cylindrical plasma geometry. The code takes account of the following physical processes using a Monte Carlo technique: Coulomb scattering between charged particles, elastic scattering between neutral particles, electron impact ionization, and charge exchange. The reliability of this code has been described in the previous paper [8] by comparing the diffusion coefficient of impurity ions with that of the classical theory. Also, it is possible to change artificially the cross-field diffusion coefficient by changing a characteristic step size of ions as follows:

$$\sqrt{\langle(\Delta r)^2\rangle} = \sqrt{2\Delta t D_\perp}, \tag{1}$$

where $D_\perp$ is the diffusion coefficient of impurity ions given artificially, and Δt is the time interval to simulate Coulomb collisions as discrete collisions in the code. The value of Δr, which is the characteristic radial step size, is calculated as a random value from a Gaussian distribution with the dispersion of $\langle(\Delta r)^2\rangle$.

From the numerical simulations spatial profiles of impurity atoms or ions emission intensity are reconstructed as follows: the light intensity in the plasma is expressed as $I_{imp} \propto N_{imp} N_e \langle \sigma_{em} v_e \rangle$, where N_{imp} and N_e are the densities of impurity and plasma electron, respectively, and $\langle \sigma_{em} v_e \rangle$ is the emmission rate coefficient determined by the electron temperature. The observation area of $\pm$20 mm $\times$ 80 mm is divided into small two-dimensional array zones. The flight of a test impurity gives the weight of $N_e \langle \sigma_{cm} v_e \rangle$ on each zone where the test impurity passes through. Many runs of such flight will give a pile up of weight which corresponds to the local emissivity.

The axial and the radial parameters of background plasma are specified by the measurement of a fast scanning Langmuir probe located at 40 cm away from the target. The ion flows come from an azimuthal $E_r \times B$ drift due to the radial potential gradient and also the axial drift along the direction of the magnetic field. The latter is estimated from one-dimensional fluid equations.

3. Results and discussions

3.1. The energy distribution of sputtered titanium

Impurity penetration into plasma increases as the velocity distribution of the ejected impurity atoms increases. We observe the decay characteristics of the atomic spectral

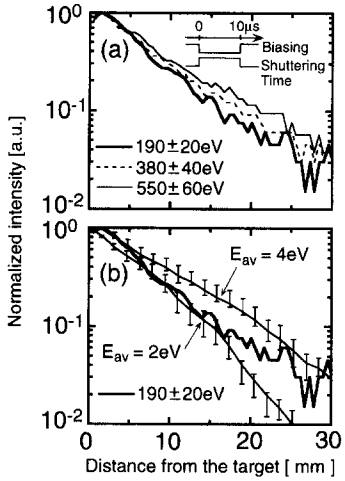

Fig. 2. Penetration characteristics for three different incident ion energy in the experiment (a) and two reconstructed profiles based on the Monte Carlo code (b) with the error bar of Langmuir probe measurements, $N_e \sim 1.5\times10^{18}$ m^{-3} and $T_e \sim 9$ eV. Thompson energy distribution and a cosine angular distribution are assumed in the simulation model.

line intensity from the target surface for three different incident ion energies as shown in Fig. 2a. The incident ion energy is determined by the voltage difference between the target and the plasma. Each line shows a sliced profile of the image experimentally obtained with the same time shuttering interval as that for the biasing pulse. This result indicates the penetration becomes deeper with the biasing voltage, therefore with the increase of incident ion energy. Reconstructed profiles based on the numerical analysis mentioned in Section 2.2 correspond with the experimental profile for the incident energy of 190 eV in Fig. 2b. The reconstructed profiles are calculated by assuming that the initial velocity of the sputtered particle is determined by the Thompson energy distribution given below [4,7] and a cosine angular distribution,

$$f(E)\,dE = \begin{cases} \dfrac{CU_0E}{(E+U_0)^3}\,dE & E \le \gamma E_{in} \\ 0 & E > \gamma E_{in} \end{cases} \qquad (2)$$

where U_0 is the surface binding energy (4.85 eV for titanium), C is a normalization constant, γ is an energy transmission factor and E_{in} is the incident ion energy. The averaged energy E_{av} is defined as follows:

$$E_{av} = \frac{\int_0^{\gamma E_{in}} Ef(E)\,dE}{\int_0^{\gamma E_{in}} f(E)\,dE}. \qquad (3)$$

The maximum energy transmission factor for helium ions on titanium target, $4M_{He}M_{Ti}/(M_{He}+M_{Ti})^2$, is 0.28, where M_{He} and M_{Ti} are the masses of helium and titanium atoms, respectively. For the incident energy of 190 eV, E_{av} is 13 eV with a maximum transfer energy of 53.2 eV, while in the experiment $E_{av} = 2 \sim 4$ eV as shown in Fig. 2b. These values are given by assuming energy transmission factors in Eq. (2). The error bars show the uncertainly range in calculation due to the error of $\pm 20\%$ in probe measurements for background plasma parameters: the electron temperature and the density are ~ 9 eV and $\sim 1.5\times10^{18}$ m^{-3}, respectively. The difference between $E_{av} = 13$ eV and $E_{av} = 2 \sim 4$ eV is caused by the high energy tail of the distribution function of sputtered particles. For low energetic ion bombardment, isotropic collision cascades do not occur sufficiently and the collisions occur only in a few atomic layers at the surface, because the conservation law of energy and momentum limits the energy transfer in an elastic collision between the two atoms.

We confirm the lack of high energy components in the energy distribution function of physically sputtered particles in a separate way. Fig. 3a shows the normalized energy distribution calculated by a particle simulation code in solid, ACAT [9]. The high energy tail of sputtered particles falls off more steeply for the incident energy of 100 eV compared with that of 300 eV. The shape of a Maxwellian velocity distribution which has the effective energy of 2.4 eV is found to be a good approximation for the incident energy of 100 eV.

Angular distributions as a function of incident energy calculated by the ACAT code are shown in Fig. 3b; which also shows their comparisons with a cosine distribution.

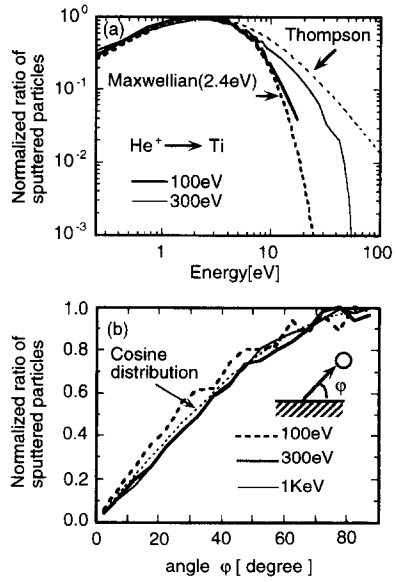

Fig. 3. Energy distributions (a) and angular distributions (b) of titanium atoms sputtered by helium bombardment at normal incidence, calculated by ACAT code taking the ion incident energy as a parameter.

The angular distributions are not so sensitive for ion bombardment energy. For instance, the distribution for the incident energy of 100 eV is equal to the under-cosine distribution of $\sim(\text{cosine})^{0.9}$. These results depend on surface conditions such as surface roughness and the coverage of oxygen [10] etc., however, such effects are not included in the present calculation of the ACAT code.

3.2. Transport of sputtered titanium in a He plasma

Fig. 4a and 4b show respectively the time evolutions of titanium atom distribution and those of ion distribution along the magnetic field. These are obtained for the incident helium ion energy of about 200 eV. The dotted lines in Fig. 4b give simulation results, using Maxwellian distribution with the temperature of 2.4 eV and a cosine angular distribution for the atomic emission from the surface. These atomic data are obtained by the comparisons of experimental observation of spatial distributions shown by the solid lines in the Fig. 4a with those determined by the code shown by the dotted line in the same figure.

Friction force induced by Coulomb collisions with plasma ions dominates the impurity ion transport along the magnetic field line, about ten times as large as electric field force and thermal force. However, such an ion flow is not easily identified experimentally because impurity ions are diffusing towards the radial direction as well as being ionized to the upper charge states. The mean life-time of impurities injected as a tracer is estimated about 42 μs by the numerical simulation, where the life-time is defined as the averaged time scale through the following processes; impurity atoms are sputtered from a plasma-facing material, ionized due to the electron impact, trapped by the magnetic field and redeposited elsewhere. This time scale agrees with that of the decrement of the light intensity.

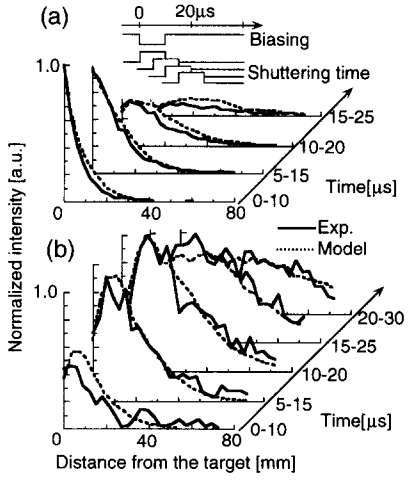

Fig. 4. Time evolutions of titanium atom (a) and ion (b) distribution along the magnetic field for different timings. Maxwellian distribution with the effective energy of 2.4 eV and a cosine distribution are assumed for ejected atoms in the simulation model. $N_e \sim 2\times10^{18}$ m^{-3} and $T_e \sim 7$ eV.

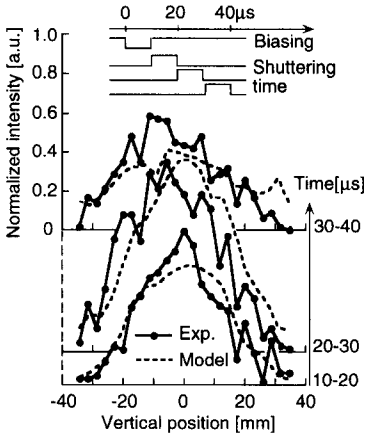

Fig. 5. Time evolution of titanium ions across the magnetic field at 5 cm away from the target. Maxwellian distribution with the effective energy of 2.4 eV and a cosine distribution for ejected atoms, and a classical cross-field diffusion are assumed in the simulation shown by dotted lines.

Fig. 5 shows the time evolution of titanium ion distribution across the magnetic field at 5 cm away from the target. We simulate the same distributions for several cross-field diffusion coefficients of $1 \sim 4$ m^2/s, and then find that the differences between the experimental profiles and numerical model appear after ~ 25 μs later from the impurity injection. By comparing the profiles ~ 25 μs later, the simulation results with the classical diffusion have an agreement with the experimentally observed time evolution of spatial Ti^+ profiles. The averaged gyroradius of Ti^+ is about 0.8 cm, and the classical $D_\perp$ is about 1 m^2/s under our experimental conditions of the helium plasma with the magnetic field of 0.13 T, the plasma density of around 2×10^{18} m^{-3} and the electron temperature of about 7 eV.

4. Conclusions

The energy distribution of physically sputtered titanium atoms is studied as a function of incident ion energy of below 600 eV. For the low bombardment energy of a few hundred eV, the averaged sputtered energy corresponds to as low as $2 \sim 4$ eV. The ACAT code gives that the energy distribution has a lack of high energy components compared with Thompson energy distribution, and the angular distribution is not so sensitive for incident ion energy.

Since the sputtered energy affects the subsequent transport and redeposition processes of impurities, we can say that it is quit important to employ a proper energy distribution of sputtered particles in a modeling analysis, especially for low incident ion energy.

Time evolution of impurity ion distributions has been obtained in the experiment. From its comparison with the numerical simulation using the velocity distribution determined by the observation of atomic spectral line, the cross-field diffusion is identified nearly as classical under our experimental conditions.

Acknowledgements

We would like to thank Dr. Y. Yamamura for providing the ACAT code. This work was supported by the Grant-in-Aid of Scientific Research from Japan Ministry of Education, Science and Culture (JSPS Fellowship, No. 0736).

References

[1] E. Vietzke, K. Flaskamp, M. Hennes and V. Philipps, Nucl. Instrum. Methods B 2 (1984) 617.
[2] H.L. Bay, B. Schweer, P. Bogen and E. Hintz, J. Nucl. Mater. 111–112 (1982) 732.
[3] P. Bogen, H.F. Döbele and Ph. Mertens, J. Nucl. Mater. 145–147 (1987) 434.
[4] M.W. Thompson, Phil. Mag. 18 (1968) 377.
[5] P. Bogen and D. Rusbüldt, J. Nucl. Mater. 196–198 (1992) 179.
[6] S. Masuzaki et al., Jpn. J. Appl. Phys. 29 (1990) 2835; Trans. IEE Jpn. 112 A (1992) 913.
[7] W. Eckstein, J. Bohdansky and J. Roth, Suppl. J. Nucl. Fusion (1991) 51.
[8] M. Kojima and S. Takamura, J. Nucl. Mater. 220–222 (1995) 1107.
[9] W. Takeuchi and Y. Yamamura, Radiation Effects 71 (1983) 53.
[10] E. Dullni, Appl. Phys. A 38 (1985) 131.